

# Investigation of Electrical and Optical Transport Properties of Annealed InO<sub>x</sub> Thin Films

M. A. Islam<sup>1,\*</sup>, R. C. Roy<sup>2</sup>, J. Hossain<sup>2</sup>, M. Julkarnain<sup>2</sup> and K. A. Khan<sup>2</sup>.

<sup>1</sup> Department of Physics, Rajshahi University of Engineering & Technology, Rajshahi-6204, Bangladesh.

<sup>2</sup> Departments of Applied Physics & Electronic Engineering, University of Rajshahi, Rajshahi-6205, Bangladesh.

Received: 12 Oct. 2015, Revised: 2 Nov. 2015, Accepted: 10 Nov. 2015.

Published online: 1 Jan. 2016.

**Abstract:** Indium oxide (InO<sub>x</sub>) films with a thickness of 50–150 nm were deposited onto glass substrate by electron beam evaporation technique. As-deposited InO<sub>x</sub> films were annealed in air at 575K for 3 hours and characterized by Scanning Electron Microscopy (SEM), electrical and optical measurements. SEM study of the film of thickness 50 nm revealed that the surfaces are distributed uniformly throughout the film with the uniform small grains. Temperature dependence of electrical resistivity was measured in the temperature range 300–475K. The decrease in resistivity with the increase of temperature indicates that InO<sub>x</sub> films are semiconducting in nature. The reduction in the resistivity with temperature might be associated with thermally activated conduction mechanism. The behavior of resistivity and so also the activation energy of annealed InO<sub>x</sub> thin films depend on thickness. From Hall study, it is observed that the films exhibit n-type electrical conductivity with carrier concentration of about 10<sup>25</sup> m<sup>-3</sup>. The absorption coefficient was calculated from the transmittance measurements. The direct optical band gap is found to vary from 3.60 to 3.72 eV as the thickness increased from 50 to 150 nm.

**Keywords:** Activation energy, Annealed, Band gap, E-beam, Thin film.

## 1 Introduction

Transparent oxide film like indium oxide (InO<sub>x</sub>) has been receiving much attention due to its transparent and conductive properties. Indium oxide has unique characteristics such as high electrical conductivity, high transparency in the visible and near-infrared spectral region, chemical stability and photochemical properties. The combination of electrical and optical properties makes InO<sub>x</sub> useful in electro-optic modulators, liquid crystal displays, solar cells, and photovoltaic devices [1-2]. It is also used as anti-reflection coating in solar cells owing to its less optical reflectivity. Furthermore, it is an attractive material used as active layers in gas sensors for ozone (O<sub>3</sub>) detection [3-4]. InO<sub>x</sub> is a wide-band-gap semiconductor (~3.70 eV) [5] which behaves as an insulator in its stoichiometric form (In<sub>2</sub>O<sub>3</sub>). A wide range of deposition techniques has been used for the preparation of InO<sub>x</sub> films, such as dc magnetron sputtering [6], evaporation [7-8], thermal oxidation of indium films [9], Pulsed laser deposition (PLD) [10-11], atomic-layer epitaxial growth [12], spin coating [13], and the sol-gel method [14], mainly in order to improve the structural and morphological properties. Electron beam evaporation is the most widely

used technique among the above-mentioned methods for deposition thin films. It deposits materials quickly. High quality films are produced by this technique.

In the previous reports the dependence of the structural, electrical and optical properties on the substrate temperature was investigated [11, 15-16]. However, it has paid relatively less attention to the study of the above mentioned properties by annealing temperature. Good opto-electronic properties achieved when these films were subjected to a heat treatment in air [17]. The conductivity of thin InO<sub>x</sub> film can be altered remarkable by post growth annealing [18-19].

In this paper, we prepared Indium oxide thin films of several thicknesses by an electron beam evaporation technique. The deposited films were then annealed at a temperature of 573K in open air and the electrical and optical properties were investigated at various thicknesses.

## 2 Experimental Details

InO<sub>x</sub> thin films were deposited on to glass substrate by e-beam evaporation technique at a pressure of 3×10<sup>-3</sup> Pa from InO<sub>x</sub> powder (99.999% pure) obtained from Aldrich Chemical Company, USA. When the chamber pressure reduced to ~ 3×10<sup>-3</sup> Pa, the deposition was then started with

\*Corresponding author E-mail: [arifapee19@gmail.com](mailto:arifapee19@gmail.com)

30 mA current by turning on the low-tension control switch. All the films were deposited at room temperature. The deposition rate was about  $5 \text{ nm s}^{-1}$ . The film thickness was measured by the Tolanasky interference method with an accuracy of  $\pm 5 \text{ nm}$  [20]. The thickness of the  $\text{InO}_x$  films ranges from 50 to 150 nm, respectively. As-deposited films were annealed by heating (temperature is changed slowly  $1 \text{ K/min}$ ) about 3 hours in open air at a temperature of  $573 \text{ K}$ . Electrical resistivity and Hall Effect measurement were investigated by the Van-der-Pauw technique [20]. The optical transmittance spectra of  $\text{InO}_x$  films were recorded from 300 nm to 1100 nm wavelength using a SHIMADZU-UV double beam spectrophotometer.

### 3 Results

#### 3.1 Morphological studies

Scanning Electron Microscope (SEM) was used to study the surface morphology of  $\text{InO}_x$  thin films. SEM micrographs of the annealed (at a temperature  $575 \text{ K}$  for 3 h in air)  $\text{InO}_x$  thin film of two different magnifications are shown in Fig.1. It shows a uniform surface morphology with a more dense homogeneous distribution of grains with well-defined boundaries.

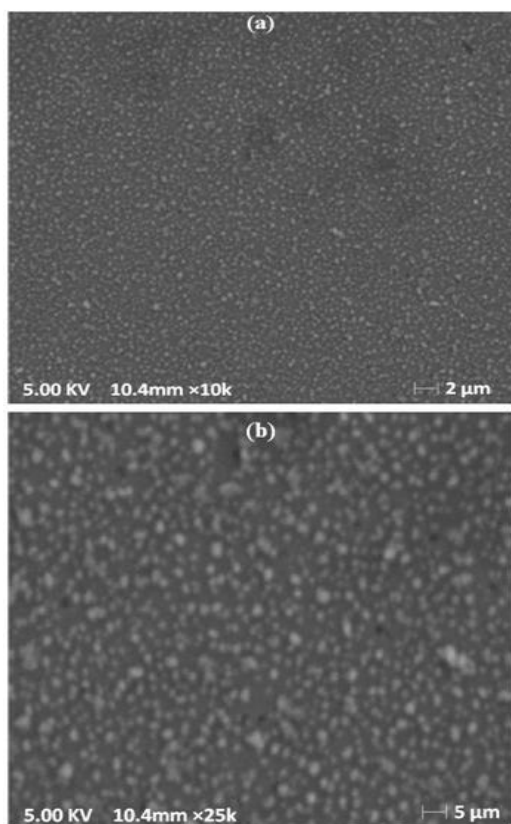


**Figure 1:** SEM micrograph of annealed  $\text{InO}_x$  thin films for a thickness of 50 nm at two magnifications.

#### 3.2 Temperature dependence of electrical conductivity and activation energy

Figure 2 shows the temperature dependence of electrical resistivity of  $\text{InO}_x$  films of different thicknesses in the temperature range  $300\text{--}475 \text{ K}$ . The resistivity decreases with increase in temperature confirms the semiconductor nature of the annealed  $\text{InO}_x$  films. This decrease in resistivity with temperature is associated with thermal activation process which leads to an increase in carrier concentration as the temperature is increased.

It is also seen from Fig. 2 that the resistivity of the films depends upon thickness, at room temperature the resistivity is found to decrease from  $15 \times 10^{-4} \text{ } (\Omega\text{-m})$  to  $7.0 \times 10^{-5} \text{ } (\Omega\text{-m})$  as the thickness increase from 50-150 nm. This decrease in resistivity with thickness can be attributed to grain boundary scattering as explained by Wu and Chiou [21]. As the grain size increases with thickness (not shown in Figure), the size of grain boundaries become relatively reduced; which in turn reduces the grain boundary scattering, consequently reducing the resistivity.

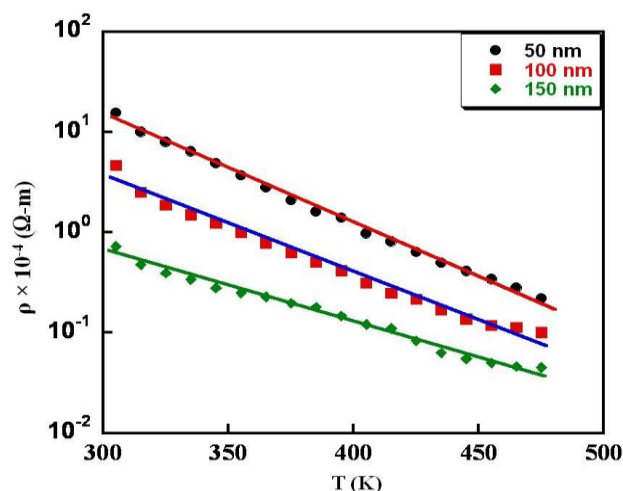


**Figure 2:** Resistivity ( $\rho$ ) of annealed  $\text{InO}_x$  thin films of three different thicknesses as a function of temperature ( $T$ ).

The activation energy is calculated by the following relation:

$$\sigma = \sigma_0 \exp(-\Delta E/2K_B T) \quad (1)$$

Where  $\Delta E$  is the activation energy,  $\sigma_0$  is the conductivity at  $0 \text{ K}$ ,  $K_B$  is the Boltzmann constant, and  $T$  is the absolute temperature. The logarithmic variation of electrical conductivity as a function of inverse temperature at several thicknesses is shown in Fig. 3(a).

The activation energies calculated from linear least square fit of Arrhenius relation. The variation of activation energy with thickness is shown in Fig. 3(b). The values of activation energies are found to be the range of  $0.62\text{--}0.41 \text{ eV}$ . It is observed that the activation energy of  $\text{InO}_x$  films decreases with increasing film thickness (Fig. 3b) which is

associated with the reduction of scattering at grain boundaries as mentioned earlier. This behaviour of activation energy with thickness also implies semiconducting behaviour of the films [22].

### 3.3 Hall Effect study

The Hall coefficient ( $R_H$ ) was calculated by the following relation [23]

$$R_H = \pm V_{Bt}/IB \text{ (m}^3/\text{coul.)} \quad (2)$$

Where  $V_B$  is the generated Hall voltage,  $t$  is the film thickness, and  $B$  is the applied magnetic field.  $R_H$  will be negative for n-type semiconductor and positive for p-type semiconductor, respectively. It is seen from the Fig.4 that Hall coefficient is negative, which indicates that  $\text{InO}_x$  sample are n-type conductivity with electrons as majority charge carriers which is well agreed with the reported value [24]. Carrier concentration is found to be the order of  $10^{25} \text{ m}^{-3}$  [25]. The following relation was used to calculate the value of carrier concentration ( $p$ ):

$$R_H = \pm 1/pe \quad (3)$$

Where  $e$  is the electronic charge.

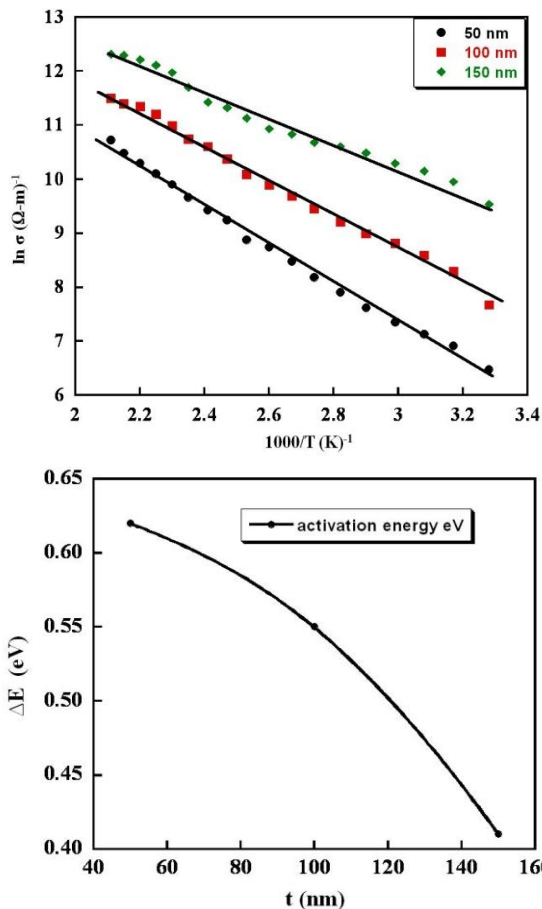


**Figure 3:** (a) Plot of  $\ln(\sigma)$  versus inverse temperature ( $1000/T$ ), (b) variation of activation energy ( $\Delta E$ ) with thickness ( $t$ ).

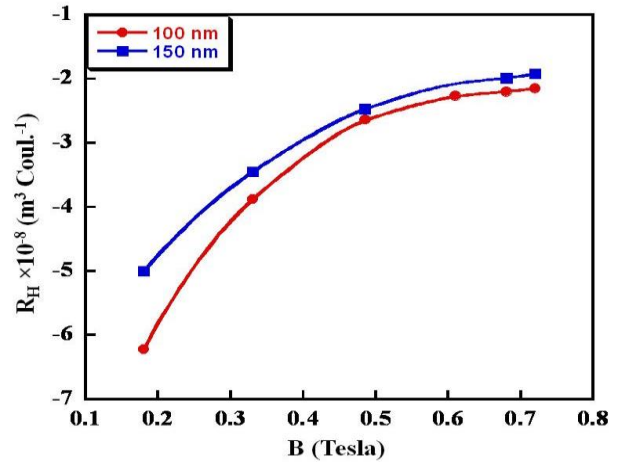


**Figure 4:** Variation of Hall coefficient ( $R_H$ ) with magnetic field ( $B$ ) of  $\text{InO}_x$  thin films.

### 3.4 Optical transmittance studies

Optical transmittance  $T$  (%) was measured at wavelength ( $\lambda$ ) range  $300 \leq \lambda \leq 1100 \text{ nm}$  using a “UV-Visible SHIMADZU double beam spectrophotometer” at room temperature. Figure 5 shows the variation of transmittance with photon wavelength of annealed  $\text{InO}_x$  thin films of different thicknesses such as 50,100 and 150 nm. It is seen that all the films are highly transparent over the visible and near-infrared regions. The films of thickness of 50 and 100nm are more transparent with average transmission of 80% in the visible region whereas, the films of thickness of 150nm are relatively less transparent with transmission of about 65 % in that region. Transmittance decreases in the higher photon energy region which may occur due to the absorption of free carriers. The absorption coefficient ( $\alpha$ ) was calculated from the transmittance ( $T$ ) measurement, using the following relation:

$$\alpha = (1/t) \ln [1/T] \quad (4)$$

Where  $t$  is film thickness in nm and  $T$  is the transmittance. Figure 6 shows the variation of absorption coefficient with photon energy of the annealed  $\text{InO}_x$  films of three different thicknesses of 50, 100, and 150 nm. The absorption coefficient for all films is found to be the order of  $10^6 \text{ m}^{-1}$ .

The absorption coefficient of  $\text{InO}_x$  films was used to calculate the energy band gap. In the fundamental absorption region, the absorption characteristics of the films described by the equation:

$$\alpha h\nu = A_0(h\nu - E_g)^{1/2} \quad (5)$$

For direct gap semiconductors, where  $h$  is Planck's constant,  $\nu$  the photon frequency,  $A_0$  a constant which depends on the transition probability, and  $E_g$  is the direct optical band gap. The plot of  $(\alpha h\nu)^2$  vs. Photon energy ( $h\nu$ ) of the annealed  $\text{InO}_x$  thin films for the different thicknesses is shown in Fig. 7. The values of the tangents, evaluated by least mean square method, intercepting the energy axis give

the values of optical band gap ( $E_g$ ). The band gap energies of the samples of three different thicknesses 50, 100, and 150 nm are 3.60, 3.66, and 3.72 eV, respectively [26].

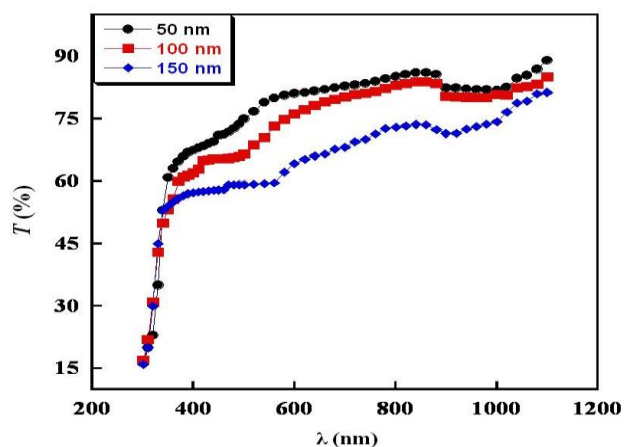


**Figure 5:** Spectral variation of transmittance ( $T$ ) of annealed InO<sub>x</sub> thin films of three different thicknesses with photon wavelength ( $\lambda$ ).

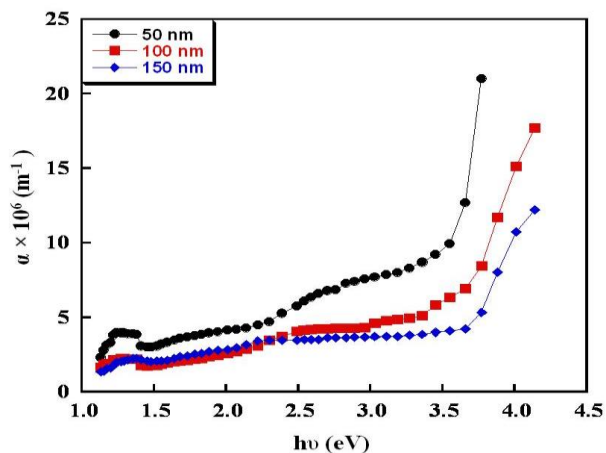


**Figure 6:** Absorption coefficient ( $\alpha$ ) vs. photon energy ( $h\nu$ ) of annealed InO<sub>x</sub> thin films.

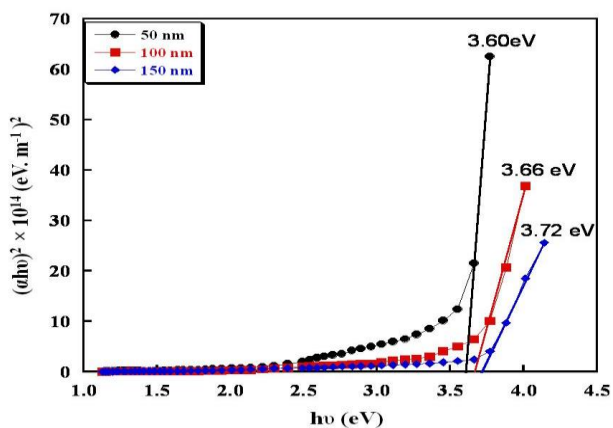


**Figure 7:** Plots of  $(\alpha h\nu)^2$  vs.  $h\nu$  of annealed InO<sub>x</sub> thin films of three different thicknesses.

## 4 Conclusions

In summary, thin films of InO<sub>x</sub> were prepared using e-beam evaporation technique at different thicknesses. The SEM micrographs of thickness 50nm show a smooth, homogenous surface morphology with relatively small grain structure. Study of electrical properties revealed semiconducting nature of the annealed InO<sub>x</sub> films. Resistivity of the thicker film is found to be comparatively less than that of thinner films. Activation energy is found to decrease as the thickness of the film increases. The films exhibit n-type conductivity with carrier concentration of about  $10^{25} \text{ m}^{-3}$ .

Thinner films show a relatively higher transmission of about 85% in the visible region and in the near infrared region. The absorption coefficient was determined from the transmittance measurements and is found to be of the order of  $10^6 \text{ m}^{-1}$ . The films show a direct allowed transition with band gap that vary in the ranges of 3.60-3.72 eV. The low resistivity of the films in conjunction with high absorption coefficient and direct optical band gap suggests that these prepared films can be considered as the suitable candidates for technological applications such as anti-reflection coating for solar cells and opto-electronic devices.

## References

- [1] C. G. Granqvist, Transparent conductive electrodes for electro chromic devices: A review, *Appl. Phys. A*: 57 (1993) 19-24.
- [2] M. Wirtz J. Kluczik, and M. Rivera, Ferredoxin-Mediated Electro catalytic Dehalogenation of Haloalkanes by Cytochrome P450cam, *J. Am. Chem. Soc.* 122 (2000) 1047-1056 .
- [3] H. Fritzsche, B. Pashmakov, and B. Clafin, Reversible changes of the optical and electrical properties of amorphous InO<sub>x</sub> by photoreduction and oxidation, *Sol. Energy Mater. Solar Cells* 32 (1994) 383-393.
- [4] G. Kiriakidis, N. Katsarakis, M. Bender, E. Gagaoudakis, and V. Cimalla, InOX Thin Films, Candidates For Novel Chemical And Optoelectronic Applications, *Mater. Phys. Mech.* 1 (2000) 83-97.
- [5] C. Xirouchaki, G. Kiriakidis, T. F. Pedersen, and H. Fritzsche, Photoreduction and oxidation of as-deposited microcrystalline indium oxide, *J. Appl. Phys.* 79 (1996) 9349.
- [6] S. Kasiviswathan, and J. Rangarajan, Direct current magnetron sputtered In<sub>2</sub>O<sub>3</sub> films as tunnel barriers, *J. Appl. Phys.* 75 (1994) 2572-2577.
- [7] S. Naseem, M. Iqbal, and K. Hussain, Opto-electrical and structural properties of evaporated indium oxide thin films, *Sol. Energy Mater. Sol. Cells* 31 (1993) 155-162.
- [8] K. G. Gopchandran, B. Joseph, J. T. Abraham, P. Koshy, and V. K. Vaidyan, The preparation of transparent electrically conducting indium oxide films by reactive



- vacuum evaporation, *Vacuum* 48 (1997) 547-550.
- [9] V. D. Das, S. Kirupavathy, L. Damodare, and N. Lakshminarayan, Optical and electrical investigations of indium oxide thin films prepared by thermal oxidation of indium thin films, *J. Appl. Phys.* 79 (1996) 8521-8530.
- [10] Y. Yamada, N. Suzuki, T. Makino, and T. Yoshida, *J. Vacuum Sci. & Tech. A*: 18 (1) 83 (2000).
- [11] F. O. Adurodija, H. Izumi, T. Ishihara, H. Yoshioka, M. Motoyama, and K. Murai, Influence of substrate temperature on the properties of indium oxide thin films, *J. Vacuum Sci. & Tech. A*: 18 (2000) 814-818.
- [12] T. Asikainen, M. Ritala, W.M. Li, R. Lappalainen, and M. Leskela, Modifying ALE grown  $\text{In}_2\text{O}_3$  films by benzoyl fluoride pulses, *Appl. Surf. Sci.* 112 (1997) 231-235
- [13] A. Gurlo, M. Ivanovskaya, A. Pfau, U. Weimar, and W. Göpel, Sol-gel prepared  $\text{In}_2\text{O}_3$  thin films, *Thin Solid Films* 307 (1997) 288-293.
- [14] S. Naseem, I. A. Rauf, and K. Hussain, Effects of oxygen partial pressure on the properties of reactively evaporated thin films of indium oxide, *Thin Solid Films* 156 (1988) 161-171.
- [15] S. Muranaka, Y. Bando, and T. Takada, Influence of substrate temperature and film thickness on the structure of reactively evaporated  $\text{In}_2\text{O}_3$  films, *Thin Solid Films* 151 (1987) 355-364.
- [16] M. Bendera, N. Katsarakis, E. Gagaoudakis, E. Hourdakakis, E. Douloufakis, V. Cimalla, and G. Kiriakidis, Dependence of the photoreduction and oxidation behavior of indium oxide films on substrate temperature and film thickness, *J. Appl. Phys.* 90 (2001) 5382-5387.
- [17] S.M. Rozati, S. Mirzapour, M.G. Takwale, B.R. Marathe, V.G. Bhide, Characterization of as-deposited and annealed indium oxide thin films, *Mat. Chem. and Phy.* 34 (1993) 119-122.
- [18] H. Morikawa and M. Fujita, Crystallization and electrical property change on the annealing of amorphous indium-oxide and indium-tin-oxide thin films, *Thin Solid Films* 359 (2000) 61-67.
- [19] M. K. Jayaraj, S. Loreti, A. Agati, and A. Parretta, Influence of Oxygen Partial Pressure and Heat Treatment on the Properties of Reactively Sputtered  $\text{In}_2\text{O}_3$  Films, *Phys. Status Solidi A*: 155 (1996) 115-123.
- [20] S. Tolansky, Multiple beam interferometry of surface and films, London: Oxford University Press, 1948.
- [21] W. Wen-Fa, C. Bi-Shiou, Effect of annealing on electrical and optical properties of RF magnetron sputtered indium tin oxide films, *Appl. Surf. Sci.* 68 (1993) 497-504.
- [22] Y. Zi-Jian, Z. Xia-Ming, W. Xiong, Z. Ying-Ying, W. Zheng-Fen, Q. Dong-Jiang, W. Hui-Zhen, D. Bin-Yang, Preparation and Characteristics of Indium Oxide Thin Films, *J. Inor. Mat.* 15 (2010) 141-144.
- [23] K. S. Ramaiah, V. S. Raja, A. K. Bhatnagar, Optical, structural and electrical properties of tin doped indium oxide thin films prepared by spray-pyrolysis technique, *Semi. Sci. & Tech.* 15 (2000) 676-683.
- [24] S. Noguchi and H. Sakata, Electrical properties of undoped  $\text{In}_2\text{O}_3$  films prepared by reactive evaporation, *J. Phys. D* 13 (1980) 1129.
- [25] K. L. Chopra, S. Major and D. K. Pandya, Transparent Conductors—A Status Review, *Thin Solid Films*, 102 (1983) 1-46
- [26] R. L. Weiher, and R. P. Ley, Optical Properties of Indium Oxide, *J. Appl. Phys.* 37 (1996) 299-302.
-